Simulation of exact quantum Ising models with a Mott insulator of paired atoms

Ren Liao,[1,*] Jingxin Sun,[1] Pengju Zhao,[2] Shifeng Yang,[1] Hui Li,[1] Xinyi Huang,[1] Wei Xiong,[1] Xiaoji Zhou,[1] Dingping Li,[2] Xiongjun Liu,[2] and Xuzong Chen[1,†]

[1]*School of Electronics, Peking University, Beijing 100871, China*

[2]*School of Physics, Peking University, Beijing 100871, China*

(Received 7 May 2022; accepted 28 September 2022; published 9 November 2022; corrected 29 November 2022)

Quantum simulation of the XXZ model with a two-component Bose- or Fermi-Hubbard model based on a Mott insulator background has been widely used in the investigations of quantum magnetism with ultracold neutral atoms. In most cases, the diagonal spin-spin interaction is always accompanied by a large spin-exchange interaction which hinders the formation of long-range magnetic order at low temperature. Here, we show that the spin-exchange interaction can be strongly reduced in a Mott insulator of paired atoms, while the diagonal spin-spin interaction remains unaffected. Thus, the effective magnetic models become the exact quantum Ising models in a one-dimensional (1D) or two-dimensional (2D) lattice. Meanwhile, we analyzed an experimentally achievable three-component Fermi-Hubbard model of ^{6}Li with two hyperfine levels of atoms paired in the lattice. We find the long-range antiferromagnetism of such a three-component Fermi-Hubbard model can be much stronger than that of a typical two-component Fermi-Hubbard model at low temperature. Our results may be useful for experimental investigations of the quantum phase transition and quantum criticality of the 1D and 2D quantum Ising models with ultracold neutral atoms.

DOI: 10.1103/PhysRevA.106.053308

I. INTRODUCTION

Quantum simulation [1] of magnetic models has made much progress in recent years. In the systems of superconducting circuits [2–6] and trapped ions [7–11], the simulated magnetic models are usually the Ising models with spatially dependent spin-spin interactions. The number of simulated spins is usually limited due to the control difficulties. Another direction is to simulate a large-scale quantum magnet in an optical lattice by controlling the long-range dipole-dipole interaction of polar gases and Rydberg atoms. It is reported that the XXZ model [12] and the antiferromagnetic Ising model [13–17] have been realized. There are also many theoretical proposals of simulating a Heisenberg-like magnetic model with polar molecules [18–21] and theoretical and experimental works about simulating magnetic models with laser-dressed Rydberg atoms [22–25]. However, the effective spin-spin interaction arising from a dipole-dipole interaction is intrinsically long range and usually inhomogeneous in the lattice. Moreover, it is typically hard to reach thermal equilibrium in the lattice due to the complexity of the dipole-dipole interaction.

Besides the dipole-dipole interaction, the superexchange interaction between neutral atoms in an optical lattice is also widely used to simulate magnetic models. The effective spin-spin interaction derived from the superexchange interaction is usually homogeneous throughout the lattice and only involves nearest-neighbor spins. Thermal equilibrium can also be reached by atom collisions in most cases. Apart from some special designs of magnetic models [26,27], the effective magnetic models are described by a XXZ model with a nearest-neighbor spin-spin interaction $J_z\hat{S}_i^z\hat{S}_j^z$ and a spin-exchange interaction $J_\perp(\hat{S}_i^+\hat{S}_j^- + \text{H.c.})$. The antiferromagnetic spin correlations of various kinds of Fermi-Hubbard models [28–34], the spin-charge separation of a hole-doped Fermi-Hubbard model [35], and the propagation of magnons [36,37] and spinons [38] have been observed with ultracold neutral atoms. However, the spin-exchange interaction is usually quite large compared with the diagonal spin-spin interaction in these XXZ models realized with neutral atoms. Though there are reported studies of simulating an exact Ising model in a tilted lattice [26,39] and a tunable XYZ model with a p-band Mott insulator [40], these methods suffer from the defect of a highly excited Mott insulator background which makes effective magnetic models unstable in the lattice.

Here, we propose a general method of simulating an Ising-like quantum magnet with the superexchange interaction of neutral atoms in an optical lattice. The main idea is to construct low-energy effective magnetic models based on a Mott insulator of paired atoms. This idea is applicable to both bosonic atoms and fermionic atoms and has broad lattice compatibility. Especially, an exact transverse Ising model with an achievable thermal equilibrium can be simulated in certain cases. The only requirement is to find suitable atom species to realize such kinds of Mott insulators without severe heating or loss caused by a three-body recombination. These features make the paired-atom Mott insulator an ideal method to simulate exact Ising models in an optical lattice.

II. THE SUPEREXCHANGE INTERACTION OF PAIRED ATOMS

To begin with, we first analyze the superexchange interaction in a Mott insulator of paired atoms. In a simplified two-

*liaoren@pku.edu.cn
†xuzongchen@pku.edu.cn

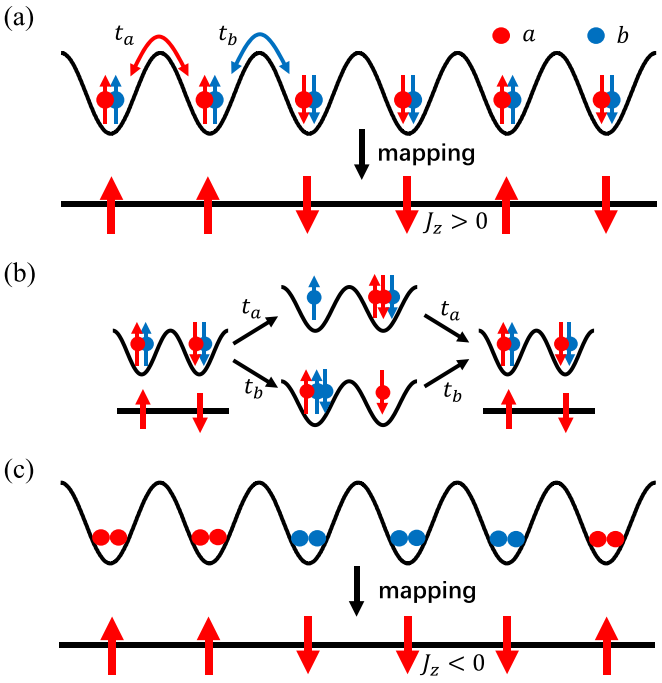

FIG. 1. (a) The low-energy effective model of a Mott insulator with spin-paired fermionic atoms is an antiferromagnetic Ising model. At each site, the same spin components of each species of atoms are paired so that $|n^a_{i\uparrow}=1, n^b_{i\uparrow}=1\rangle$ and $|n^a_{i\downarrow}=1, n^b_{i\downarrow}=1\rangle$ can be mapped to spin up and down of a single spin, respectively. (b) The second-order low-energy superexchange interaction between spin-paired fermions. It can be seen that the spin-exchange terms are prohibited. (c) The Mott insulator of paired bosonic atoms generates an effective ferromagnetic Ising model when the on-site repulsive interaction of heteronuclear atom pairs U^{ab} is larger than those of homonuclear atom pairs U_a, U_b.

species two-spin Fermi-Hubbard model shown in Fig. 1(a), the Hamiltonian can be written as

$$\begin{aligned}\hat{H}^{\rm FH}_{\rm pair} &= \hat{H}^{\rm FH}_a + \hat{H}^{\rm FH}_b + \hat{H}^{\rm FH}_{ab},\\ \hat{H}^{\rm FH}_{s=a,b} &= -t_s \sum_{\sigma=\uparrow\downarrow}\sum_{\langle ij\rangle}(\hat{s}^\dagger_{i\sigma}\hat{s}_{j\sigma} + {\rm H.c.}) + U_s\sum_i \hat{n}^s_{i\uparrow}\hat{n}^s_{i\downarrow}\\ &\quad - t_{xs}\sum_i(\hat{s}^\dagger_{i\uparrow}\hat{s}_{j\downarrow} + {\rm H.c.}) + \delta_{zs}\sum_i\left(\hat{n}^s_{i\uparrow} - \hat{n}^s_{i\downarrow}\right),\\ \hat{H}^{\rm FH}_{ab} &= -U^{ab}\sum_{\sigma=\uparrow\downarrow}\sum_i \hat{n}^a_{i\sigma}\hat{n}^b_{i\sigma}. \end{aligned} \tag{1}$$

Here, $\langle ij\rangle$ represents the nearest-neighbor sites. The parameters are set as $t_s, t_{xs}, \delta_{zs} \ll U_a, U_b, U^{ab}$ $(s=a,b)$. At the half-filling regime for each species of atoms, large U_a, U_b requires each lattice site to be filled with only one a atom and one b atom. U^{ab} provides a strong pairing interaction between the same spin components of a, b atoms so that there are only two possible occupation states $|\hat{n}^a_{i\uparrow}=1, \hat{n}^b_{i\uparrow}=1\rangle$ and $|\hat{n}^a_{i\downarrow}=1, \hat{n}^b_{i\downarrow}=1\rangle$ for the lowest-energy subspace, which can be mapped to $|\hat{S}^z_i = 1/2\rangle$ and $|\hat{S}^z_i = -1/2\rangle$ of a single $S=1/2$ spin, respectively. Up to second-order perturbations, the low-energy effective spin model of $\hat{H}^{\rm FH}_{\rm pair}$ can be written as

$$\hat{H}^{\rm FH}_{\rm eff} = J^{\rm FH}_z\sum_{\langle ij\rangle}\hat{S}^z_i\hat{S}^z_j - h^{\rm FH}_x\sum_i\hat{S}^x_i + h^{\rm FH}_z\sum_i\hat{S}^z_i, \tag{2}$$

with $J^{\rm FH}_z = \sum_s \frac{4t_s^2}{U^{ab}+U_s}$, $h^{\rm FH}_x = \frac{4t_{xa}t_{xb}}{U^{ab}}$, $h^{\rm FH}_z = 2(\delta_{za}+\delta_{zb})$. Comparing with the typical two-component Fermi-Hubbard model of generating a low-energy effective Heisenberg model [41], we could find the spin-pairing interaction $\hat{H}_{ab}$ is the key factor for the realization of an exact Ising model [Fig. 1(b)].

When we consider a Mott insulator of two species of bosonic atom pairs as shown in Fig. 1(c), the Hamiltonian of such a Bose-Hubbard model can be given as

$$\begin{aligned}\hat{H}^{\rm BH}_{\rm pair} &= \hat{H}^{\rm BH}_a + \hat{H}^{\rm BH}_b + \hat{H}^{\rm BH}_{ab},\\ \hat{H}^{\rm BH}_{s=a,b} &= -t_s\sum_{\langle ij\rangle}(\hat{s}^\dagger_i\hat{s}_j + {\rm H.c.}) + \sum_i\frac{U_s}{2}\hat{n}_{is}(\hat{n}_{is}-1),\\ \hat{H}^{\rm BH}_{ab} &= U^{ab}\sum_i\hat{n}_{ia}\hat{n}_{ib} - t_{ab}\sum_i(\hat{a}^\dagger_i\hat{b}_i + {\rm H.c.}). \end{aligned} \tag{3}$$

Here, $\hat{s}^\dagger_i, \hat{s}_i$ $(s=a,b)$ become bosonic operators. The parameters satisfy $t_s, t_{ab}, |U_a - U_b| \ll U_s, U^{ab} - U_s$ $(s=a,b)$. With the same spin mapping in Fig. 1(c), the effective Hamiltonian becomes

$$\hat{H}^{\rm BH}_{\rm eff} = J^{\rm BH}_z\sum_{\langle ij\rangle}\hat{S}^z_i\hat{S}^z_j - h^{\rm BH}_x\sum_i\hat{S}^x_i + h^{\rm BH}_z\sum_i\hat{S}^z_i, \tag{4}$$

with

$$J^{\rm BH}_z = \sum_{s=a,b}\left[\frac{4t_s^2}{2U^{ab}-U_s} - \frac{12t_s^2}{U_s}\right], \quad h^{\rm BH}_x = \sum_{s=a,b}\frac{2t_{ab}^2}{U^{ab}-U_s},$$

$$h^{\rm BH}_z = U_a - U_b + \frac{12t_b^2}{U_b} - \frac{12t_a^2}{U_a}.$$

Here, we ignored the boundary differences. It can be seen that $J^{\rm BH}_z < 0$ so that the ferromagnetic Ising model can also be exactly simulated. It is also noticeable that the magnitude of $|J^{\rm BH}_z|$ can be several times larger than a typical superexchange interaction with a magnitude $4t^2/U$. If such a model can be implemented in experiment, the requirement of a low-spin temperature to observe the magnetic order induced by a superexchange interaction can be strongly relieved.

III. THE THREE-COMPONENT FERMI-HUBBARD MODEL

Equations (1) and (3) provide two ideal models of simulating an exact Ising model with a Hubbard model. However, when considering the experimental realization of $\hat{H}^{\rm FH}_{\rm pair}$ and $\hat{H}^{\rm BH}_{\rm pair}$, there are two non-negligible concerns which need to be taken into account. One is the three-body recombination which may cause serious atom loss or heating in the lattice. The other is the realization of U^{ab} should be in accordance with U_a and U_b, considering the on-site interactions are mainly tuned with Feshbach resonance by controlling the s-wave scattering length $a_{ss'}(B)$ (s, s' are the same or two different atoms) with a magnetic field B [42]. However, there are six different $a_{ss'}(B)$ curves between the four different atoms in Fig. 1(a)

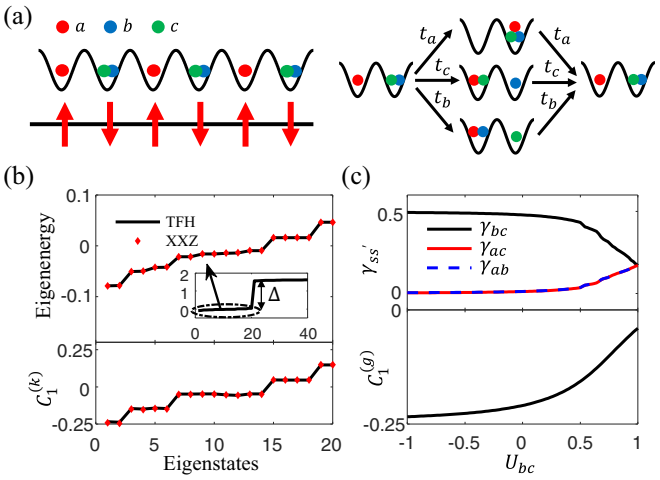

FIG. 2. The three-component Fermi-Hubbard model (TFH model). (a) Spin up and down can be represented by a atoms and b, c atom pairs in each lattice site, respectively. (b) The eigenenergy spectrum and the nearest-neighbor spin correlations $C_1^{(k)}$ of the lowest $N_S = 20$ eigenstates of the TFH model are both consistent with those of the effective XXZ model. Here, k is the index of eigenstates. The parameters are set as $t_a = t_b = t_c = 1/7$, $U_{ab} = U_{ac} = -U_{bc} = 1$, $N_a = N_b = N_c = 3$, $L = 6$. (c) The effective nearest-neighbor spin correlation $C_1^{(g)}$ and the pairing ratios $\gamma_{ss'}$ ($ss' = ab, bc, ac$) of the ground state with respect to U_{bc}. When U_{bc} is decreased from $U_{bc} = 1$ to $U_{bc} = -1$, an antiferromagnetic ground state comes into existence gradually ($C_1^{(g)} \to -1/4$) as b, c atoms begin to be paired ($\gamma_{bc} \to 0.5$, $\gamma_{ab} \to 0$, $\gamma_{ac} \to 0$).

and three different $a_{ss'}(B)$ curves for the bosonic case, while the tuning parameter is only the magnetic field B. $\hat{H}_{\text{pair}}^{\text{FH}}$ is nearly impossible to be realized while $\hat{H}_{\text{pair}}^{\text{BH}}$ can be possibly realized with certain atom species. For example, it is possible to simulate $\hat{H}_{\text{pair}}^{\text{BH}}$ with a mixture of ^{87}Rb $|F = 1, m_F = -1\rangle$ (denoted as a atoms) and ^{85}Rb $|F = 2, m_F = -2\rangle$ (denoted as b atoms) considering $a_{aa} = 100.4a_0$ [43], $a_{bb} = -443a_0[1 - 10.7/(B - 155.04)]$ [44], and $a_{ab} = 213a_0[1 - 5.8/(B - 265.4)]$ [45]. Under a magnetic field of around $B = 163.8$ G, $a_{aa} = 100.4a_0$, $a_{bb} = 100.6a_0$, and $a_{ab} = 225.2a_0$ can be obtained. Here, a_0 is the Bohr radius. Since a_{aa} and a_{ab} are quite insensitive to B when $B < 200$ G, it is very easy to tune $a_{aa} - a_{bb}$ at around $B = 163$–165 G.

Meanwhile, to indicate the experimental feasibility of a paired-atom Mott insulator with fermionic atoms, we introduce a three-component Fermi-Hubbard model (TFH model) shown in Fig. 2(a),

$$\hat{H} = -\sum_{\langle ij\rangle}\sum_{s=a,b,c} t_s(\hat{s}_i^{\dagger}\hat{s}_j + \text{H.c.}) + \sum_i \sum_{s\neq s'} U_{ss'}\hat{n}_{is}\hat{n}_{is'}. \quad (5)$$

Here, t_a, t_b, t_c are the tunneling energy of each species of atoms and $U_{ss'}$ ($ss' = ab, ac, bc$) are the on-site interactions between different atom pairs in each site. We assume each lattice site is filled with either an a atom or a b, c atom pair and the number of each species of atoms is half the number of lattice sites N_{site}. The parameters satisfy $t_a, t_b, t_c \ll U_{ac} - U_{bc}, U_{ab} - U_{bc}, U_{ac} + U_{ab} + U_{bc}$. Thus, $|\hat{n}_{ia} = 1\rangle$ and $|\hat{n}_{ib} = 1, \hat{n}_{ic} = 1\rangle$ can be mapped to spin up and down for the lowest-energy subspace [Fig. 2(a)], respectively. The low-

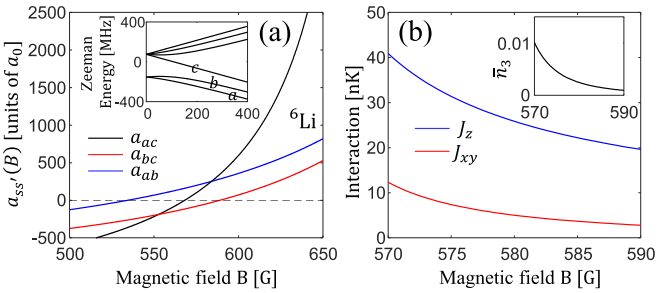

FIG. 3. Realization of the TFH model with ^{6}Li atoms. (a) The lowest three hyperfine levels of ^{6}Li can just be mapped to the a, b, c atoms required in Fig. 2(a). The s-wave scattering lengths $a_{ss'}$ ($ss' = ab, ac, bc$) of ^{6}Li satisfy $a_{ab}, a_{ac} > 0$, $a_{bc} < 0$ when 570 G $\leqslant B \leqslant$ 590 G, and the three-body recombination rate of a, b, c atoms reaches a minimum at around $B = 560$–590 G [46,47]. (b) The estimated magnetic interaction J_z, J_{xy} of the TFH model based on the experimental parameters of the Fermi-Hubbard model realized with ^{6}Li [33]. Here, we assume $U_{ss'}(B) = a_{ss'}(B)/210a_0 * 6.50$ kHz, $t_a = t_b = t_c = 0.90$ kHz. The inset is the mean three-body occupation $\bar{n}_3$ of the lowest N_S eigenstates in Fig. 2(b) per lattice site calculated in a 1D lattice with $L = 6$.

energy effective model in a cubic lattice can be written as

$$\hat{H}_{\text{eff}} = \sum_{\langle ij\rangle} J_z\hat{S}_{iz}\hat{S}_{jz} - J_{xy}(\hat{S}_{ix}\hat{S}_{jx} + \hat{S}_{iy}\hat{S}_{jy}). \quad (6)$$

Here, $J_z = \sum_{s=a,b,c}\frac{2t_s^2}{U_{s2}}$ and $J_{xy} = \frac{4t_at_bt_c}{U_{a2}U_{b2}} + \frac{4t_at_bt_c}{U_{a2}U_{c2}} + \frac{4t_at_bt_c}{U_{b2}U_{c2}}$ with $U_{a2} = U_{ab} + U_{ac}$, $U_{b2} = U_{ab} - U_{bc}$, $U_{c2} = U_{ac} - U_{bc}$. J_{xy} comes from the third-order perturbative terms and $J_{xy} \ll J_z$.

To make a quantitative study of the TFH model, we calculate the eigenenergy spectrum and the nearest-neighbor spin correlations $C_1^{(k)} = \sum_{i=1}^{L-1}\langle\psi_k|\hat{S}_{iz}\hat{S}_{i+1,z}|\psi_k\rangle/(L-1)$ of the lowest $N_S = \frac{L!}{N_a!(L-N_a)!}$ eigenstates of $\hat{H}$ under $U_{ab} = U_{ac} = -U_{bc} = 1$, $t_a = t_b = t_c = 1/7$. Here, $|\psi_k\rangle$ is the kth lowest eigenstate of $\hat{H}$, and $L = 6$ and $N_a = L/2$ are the lattice length and the number of a atoms in our numerical calculation, respectively. The results show good consistency of the eigenenergy spectrum and the nearest-neighbor correlation functions of $\hat{H}_{\text{eff}}$ [Fig. 2(b)]. There is also a large energy gap Δ ($\Delta \gg J_z$) above the lowest N_S eigenstates so that the partition function of the TFH model $Z = \text{tr}(e^{-\hat{H}/k_BT}) \approx \text{tr}(e^{-\hat{H}_{\text{eff}}/k_BT})$ when k_BT is at the same order as J_z. Meanwhile, to validate the relation between a reduced spin-exchange interaction and the pairing of b, c atoms, we calculate the spin correlation $C_1^{(g)} = \sum_{i=1}^{L-1}\langle\psi_g|\hat{S}_{iz}\hat{S}_{i+1,z}|\psi_g\rangle/(L-1)$ and the pairing ratio between different species of atoms $\gamma_{ss'} = \sum_{i=1}^{L}\langle\psi_g|\hat{n}_{is}\hat{n}_{is'}|\psi_g\rangle/L$ ($ss' = ab, ac, bc$) of the ground state $|\psi_g\rangle$ of $\hat{H}$ at different U_{bc}. It can be seen that $C_1^{(g)}$ approaches to $-1/4$ while $\gamma_{bc} \to 0.5$, $\gamma_{ab} \to 0$, $\gamma_{ac} \to 0$ when U_{bc} is decreased from $U_{bc} = 1$ to $U_{bc} = -1$ [Fig. 2(c)], validating the reduced spin-exchange interaction is due to the pairing of b, c atoms.

For the possible experimental realization of the TFH model, the a, b, c atoms can just be represented by the lowest three hyperfine levels of ^{6}Li [Fig. 3(a)]. The three-body loss feature of the lowest three hyperfine levels of ^{6}Li has been widely investigated experimentally [46–48]. In the range of about $B = 560$–590 G, the three-body recombination rate

K_3 reaches a minimum $K_{3,\min} \approx 10^{-25}$ cm^3/s [46,47]. In this magnetic range, $a_{ss'}$ is at the order of hundreds of Bohr radius and the bound states of a, b, c atoms with positive $a_{ss'}$ are sufficiently deep so that the atom-dimer coupling can be safely ignored. In this way, the mixture of a, b, c atoms in an optical lattice can just be described by the TFH model. If the lattice is filled as shown in Fig. 2(a), the three-body loss rate of a, b, c atoms in each lattice site can be roughly estimated as $\Gamma_{\rm loss} = K_3\langle\hat{n}_3\rangle/a_{\rm lat}^6$ [46,49]. Here, $a_{\rm lat}$ is the lattice constant and $\langle\hat{n}_3\rangle = \sum_i\langle\hat{n}_{ia}\hat{n}_{ib}\hat{n}_{ic}\rangle/N_{\rm site}$ is the mean three-body occupation number in each lattice site. The estimated mean three-body occupation number $\bar{n}_3 = N_S^{-1}\sum_{k=1}^{N_S}\langle\hat{n}_3\rangle_k$ of the lowest N_S eigenstates in Fig. 2(b) is evaluated under a proper selection of parameters [Fig. 3(b)]. It can be seen that $\bar{n}_3$ is quite small for the lowest N_S eigenstates when the on-site interaction of a three-body occupation is high. If we make an approximation $\langle\hat{n}_3\rangle \approx 0.01$, $a_{\rm lat} = 532$ nm, the loss rate per lattice site will be $\Gamma_{\rm loss} \approx 0.04$ Hz. For a lattice with $N_{\rm site} \approx 100$, the three-body loss rate is at the order of several Hz. Therefore, the Mott insulator of a, b, c atoms [Fig. 2(a)] can be stable in a timescale of hundreds of milliseconds. For a tunneling energy at the order of hundreds of Hz, it is long enough for the experimental observation of the antiferromagnetic order under thermal equilibrium before severe atom loss.

Another concern is the magnitude of J_z and J_{xy} which determines the magnitude of the required temperature. In the realization of the typical two-component Fermi-Hubbard model with ^{6}Li [33], $a_{ab} = 210a_0$, $t = 0.90$ kHz, $U = 6.50$ kHz can be achieved in a lattice of $V_{\rm lat} = 7.4E_R$, $a_{\rm lat} = 569$ nm under a magnetic field of $B = 576$ G. Here, $V_{\rm lat}$ is the lattice depth and E_R is the recoil energy. This yields an effective Heisenberg model $J\sum_{\langle ij\rangle}\mathbf{S}_i\cdot\mathbf{S}_j$ with $J = 4t^2/U = 0.50$ kHz $= 24$ nK. Here, we set the Planck constant and the Boltzmann constant to unity for simplicity hereafter. To make a proper estimate of the magnitude of experimentally accessible J_z and J_{xy}, we assume the TFH model is realized in the same lattice configuration as in Ref. [33]. Accordingly, $t_a = t_b = t_c = 0.90$ kHz, $U_{ss'}(B) = a_{ss'}(B)/210a_0 * 6.5$ kHz can be estimated if the magnetic field is near 576 G. Under such a selection of parameters, $t_a, t_b, t_c \ll U_{ab} - U_{bc}, U_{ac} - U_{bc}, U_{ac} + U_{ab} + U_{bc}$ can be maintained in 570 G $< B <$ 590 G so that the mapping to $\hat{H}_{\rm eff}$ is always valid. The estimated J_z, J_{xy} are shown in Fig. 3(b). It can be seen that J_z can be improved while J_{xy} is largely reduced. Especially, $J_z = 29$ nK, $J_{xy} = 6.3$ nK can be achieved with $U_{ab} = 6.5$ kHz, $U_{ac} = 4.1$ kHz, $U_{bc} = -2.1$ kHz at $B = 576$ G.

To quantitatively evaluate the antiferromagnetism of the TFH model and the Fermi-Hubbard model (FH model), we calculate the effective spin correlation and the staggered magnetization

$$C_{\mathbf{d}} = \frac{1}{N_{\mathbf{d}}}\sum_{\mathbf{r}}\langle\hat{S}^z_{\mathbf{r}}\hat{S}^z_{\mathbf{r}+\mathbf{d}}\rangle, \quad m_z = \sqrt{\left\langle\sum_{\mathbf{r}}(-1)^{x+y}\hat{S}^z_{\mathbf{r}}/N_{\rm site}\right\rangle^2}, \tag{7}$$

of the TFH model and the FH model in a 3×3 lattice. Here, $\mathbf{r} = (x, y)$ and $\mathbf{d} = (d_x, d_y)$ and $N_{\mathbf{d}}$ is the number of allowed $\hat{S}^z_{\mathbf{r}}\hat{S}^z_{\mathbf{r}+\mathbf{d}}$. From Figs. 4(a) and 4(b), it can be seen that the antiferromagnetism of the TFH model is much closer to the Ising model instead of the Heisenberg model. In addition, the antiferromagnetism of the TFH model is apparently enhanced in the low-temperature limit ($T \leqslant 20$ nK), especially, much stronger than that of the FH model when T reaches below 5 nK.

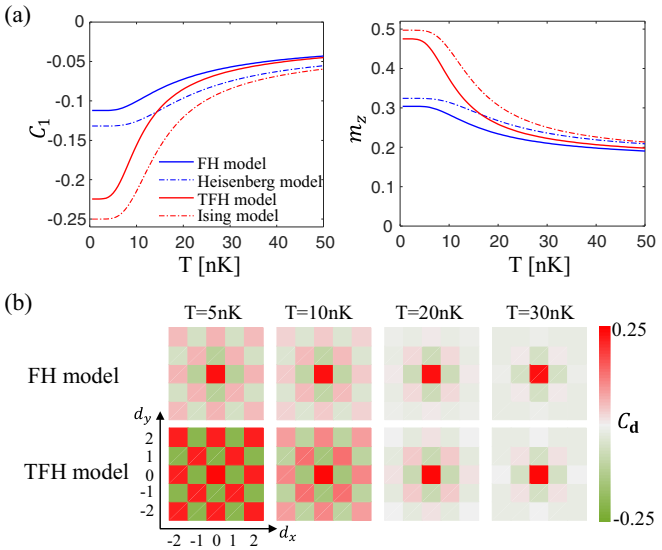

FIG. 4. Enhanced antiferromagnetism of the three-component Fermi-Hubbard model (TFH model) compared with the two-component Fermi-Hubbard model (FH model). (a) The nearest-neighbor spin correlation C_1 and the staggered magnetization m_z of the FH model ($J^{\rm eff} = 24$ nK), the Heisenberg model ($J = 24$ nK), the TFH model ($J_z^{\rm eff} = 29$ nK, $J_{xy}^{\rm eff} = 6.3$ nK), and the Ising model ($J_z = 29$ nK) in a 3×3 lattice. The parameters of the TFH model are assumed to be $t_a = t_b = t_c = 0.90$ kHz, $U_{ss'}(B) = a_{ss'}(B)/210a_0 * 6.5$ kHz (with $B = 576$ G) according to the parameters $t = 0.90$ kHz, $U = 6.5$ kHz of the FH model realized with ^{6}Li [33]. (b) The long-range spin correlations $C_{\mathbf{d}}$ of the FH model and the TFH model. It can be seen that the antiferromagnetism of the TFH model is apparently enhanced compared with the FH model when $T \leqslant 20$ nK.

IV. CONCLUSION AND OUTLOOK

In summary, we have analyzed a general scheme to simulate the quantum Ising models driven by a superexchange interaction in a Mott insulator of paired atoms. Compared with other methods of simulating an Ising model, this method features homogeneous nearest-neighbor spin-spin interactions, broad lattice compatibility, and achievable thermal equilibrium. Also, we showed the enhanced antiferromagnetism of an experimentally achievable three-component Fermi-Hubbard model of ^{6}Li with two hyperfine levels of atoms paired. Similar ideas can be applied to other mixtures of atoms. Meanwhile, it is also very promising to realize $\hat{H}_{\rm pair}^{\rm BH}$ to simulate an exact 2D transverse Ising model experimentally. Since the exact analytical solution of a 3D Ising model, which can be mapped to the 2D transverse Ising model by quantum-classical mapping [50], is still beyond theoretical reach [51], it may promote the research of this problem by experimentally realizing an exact 2D transverse Ising model. Our results may be useful for experimental investigations of the quantum Ising models with ultracold neutral atoms.

ACKNOWLEDGMENT

This work is supported by the National Natural Science Foundation of China (Grants No. 11920101004, No. 11334001, No. 61727819, No. 61475007, and No. 11825401), and the National Key Research and Development Program of China (Grants No. 2021YFA1400900 and No. 2021YFA0718300).

[1] I. M. Georgescu, S. Ashhab, and F. Nori, Rev. Mod. Phys. **86**, 153 (2014).
[2] Y. Salathe, M. Mondal, M. Oppliger, J. Heinsoo, P. Kurpiers, A. Potocnik, A. Mezzacapo, U. LasHeras, L. Lamata, E. Solano, S. Filipp, and A. Wallraff, Phys. Rev. X **5**, 021027 (2015).
[3] M. Gong, X. Wen, G. Sun, D.-W. Zhang, D. Lan, Y. Zhou, Y. Fan, Y. Liu, X. Tan, H. Yu, Y. Yu, S.-L. Zhu, S. Han, and P. Wu, Sci. Rep. **6**, 22667 (2016).
[4] R. Barends, A. Shabani, L. Lamata, J. Kelly, A. Mezzacapo, U. L. Heras, R. Babbush, A. G. Fowler, B. Campbell, Y. Chen, Z. Chen, B. Chiaro, A. Dunsworth, E. Jeffrey, E. Lucero, A. Megrant *et al.*, Nature (London) **534**, 222 (2016).
[5] R. Harris, Y. Sato, A. J. Berkley, M. Reis, F. Altomare, M. H. Amin, K. Boothby, P. Bunyk, C. Deng, C. Enderud, S. Huang, E. Hoskinson, M. W. Johnson, E. Ladizinsky, N. Ladizinsky *et al.*, Science **361**, 162 (2018).
[6] A. Cervera-Lierta, Quantum **2**, 114 (2018).
[7] A. Friedenauer, H. Schmitz, J. T. Glueckert, D. Porras, and T. Schaetz, Nat. Phys. **4**, 757 (2008).
[8] K. Kim, M.-S. Chang, S. Korenblit, R. Islam, E. E. Edwards, J. K. Freericks, G.-D. Lin, L.-M. Duan, and C. Monroe, Nature (London) **465**, 590 (2010).
[9] K. Kim, S. Korenblit, R. Islam, E. E. Edwards, M.-S. Chang, C. Noh, H. Carmichael, G.-D. Lin, L.-M. Duan, C. C. J. Wang, J. K. Freericks, and C. Monroe, New J. Phys. **13**, 105003 (2011).
[10] B. P. Lanyon, C. Hempel, D. Nigg, M. Müller, R. Gerritsma, F. Zähringer, P. Schindler, J. T. Barreiro, M. Rambach, G. Kirchmair, M. Hennrich, P. Zoller, R. Blatt, and C. F. Roos, Science **334**, 57 (2011).
[11] J. W. Britton, B. C. Sawyer, A. C. Keith, C.-C. J. Wang, J. K. Freericks, H. Uys, M. J. Biercuk, and J. J. Bollinger, Nature (London) **484**, 489 (2012).
[12] A. de Paz, A. Sharma, A. Chotia, E. Marechal, J. H. Huckans, P. Pedri, L. Santos, O. Gorceix, L. Vernac, and B. Laburthe-Tolra, Phys. Rev. Lett. **111**, 185305 (2013).
[13] E. Guardado-Sanchez, P. T. Brown, D. Mitra, T. Devakul, D. A. Huse, P. Schauss, and W. S. Bakr, Phys. Rev. X **8**, 021069 (2018).
[14] H. Labuhn, D. Barredo, S. Ravets, S. de Léséleuc, T. Macrì, T. Lahaye, and A. Browaeys, Nature (London) **534**, 667 (2016).
[15] P. Schauss, Quantum Sci. Technol. **3**, 023001 (2018).
[16] G. Semeghini, H. Levine, A. Keesling, S. Ebadi, T. T. Wang, D. Bluvstein, R. Verresen, H. Pichler, M. Kalinowski, R. Samajdar, A. Omran, S. Sachdev, A. Vishwanath, M. Greiner, V. Vuletic, and M. D. Lukin, Science **374**, 1242 (2021).
[17] P. Scholl, M. Schuler, H. J. Williams, A. A. Eberharter, D. Barredo, K.-N. Schymik, V. Lienhard, L.-P. Henry, T. C. Lang, T. Lahaye, A. M. Läuchli, and A. Browaeys, Nature (London) **595**, 233 (2021).
[18] R. Barnett, D. Petrov, M. Lukin, and E. Demler, Phys. Rev. Lett. **96**, 190401 (2006).
[19] A. V. Gorshkov, S. R. Manmana, G. Chen, J. Ye, E. Demler, M. D. Lukin, and A. M. Rey, Phys. Rev. Lett. **107**, 115301 (2011).
[20] A. V. Gorshkov, S. R. Manmana, G. Chen, E. Demler, M. D. Lukin, and A. M. Rey, Phys. Rev. A **84**, 033619 (2011).
[21] K. R. A. Hazzard, S. R. Manmana, M. Foss-Feig, and A. M. Rey, Phys. Rev. Lett. **110**, 075301 (2013).
[22] A. W. Glaetzle, M. Dalmonte, R. Nath, C. Gross, I. Bloch, and P. Zoller, Phys. Rev. Lett. **114**, 173002 (2015).
[23] J. Zeiher, R. van Bijnen, P. Schauß, S. Hild, J.-y. Choi, T. Pohl, I. Bloch, and C. Gross, Nat. Phys. **12**, 1095 (2016).
[24] F. Yang, S. Yang, and L. You, Phys. Rev. Lett. **123**, 063001 (2019).
[25] S. Hollerith, K. Srakaew, D. Wei, A. Rubio-Abadal, D. Adler, P. Weckesser, A. Kruckenhauser, V. Walther, R. van Bijnen, J. Rui, C. Gross, I. Bloch, and J. Zeiher, Phys. Rev. Lett. **128**, 113602 (2022).
[26] J. Simon, W. S. Bakr, R. Ma, M. E. Tai, P. M. Preiss, and M. Greiner, Nature (London) **472**, 307 (2011).
[27] J. Struck, C. Olschlager, R. L. Targat, P. Soltan-Panahi, A. Eckardt, M. Lewenstein, P. Windpassinger, and K. Sengstock, Science **333**, 996 (2011).
[28] D. Greif, T. Uehlinger, G. Jotzu, L. Tarruell, and T. Esslinger, Science **340**, 1307 (2013).
[29] R. A. Hart, P. M. Duarte, T.-L. Yang, X. Liu, T. Paiva, E. Khatami, R. T. Scalettar, N. Trivedi, D. A. Huse, and R. G. Hulet, Nature (London) **519**, 211 (2015).
[30] M. Boll, T. A. Hilker, G. Salomon, A. Omran, J. Nespolo, L. Pollet, I. Bloch, and C. Gros, Science **353**, 1257 (2016).
[31] L. W. Cheuk, M. A. Nichols, K. R. Lawrence, M. Okan, H. Zhang, E. Khatami, N. Trivedi, T. Paiva, M. Rigol, and M. W. Zwierlein, Science **353**, 1260 (2016).
[32] J. H. Drewes, L. A. Miller, E. Cocchi, C. F. Chan, N. Wurz, M. Gall, D. Pertot, F. Brennecke, and M. Kohl, Phys. Rev. Lett. **118**, 170401 (2017).
[33] A. Mazurenko, C. S. Chiu, G. Ji, M. F. Parsons, M. Kanász-Nagy, R. Schmidt, F. Grusdt, E. Demler, D. Greif, and M. Greiner, Nature (London) **545**, 462 (2017).
[34] H. Ozawa, S. Taie, Y. Takasu, and Y. Takahashi, Phys. Rev. Lett. **121**, 225303 (2018).
[35] T. A. Hilker, G. Salomon, F. Grusdt, A. Omran, M. Boll, E. Demler, I. Bloch, and C. Gross, Science **357**, 484 (2017).
[36] I. Dimitrova, N. Jepsen, A. Buyskikh, A. Venegas-Gomez, J. Amato-Grill, A. Daley, and W. Ketterle, Phys. Rev. Lett. **124**, 043204 (2020).
[37] T. Fukuhara, P. Schauß, M. Endres, S. Hild, M. Cheneau, I. Bloch, and C. Gross, Nature (London) **502**, 76 (2013).
[38] J. Vijayan, P. Sompet, G. Salomon, J. Koepsell, S. Hirthe, A. Bohrdt, F. Grusdt, I. Bloch, and C. Gross, Science **367**, 186 (2020).

[39] R. Liao, F. Xiong, and X. Chen, Phys. Rev. A **103**, 043312 (2021).
[40] F. Pinheiro, G. M. Bruun, J.-P. Martikainen, and J. Larson, Phys. Rev. Lett. **111**, 205302 (2013).
[41] E. Manousakis, Rev. Mod. Phys. **63**, 1 (1991).
[42] C. Chin, R. Grimm, P. Julienne, and E. Tiesinga, Rev. Mod. Phys. **82**, 1225 (2010).
[43] K. M. Mertes, J. W. Merrill, R. Carretero-González, D. J. Frantzeskakis, P. G. Kevrekidis, and D. S. Hall, Phys. Rev. Lett. **99**, 190402 (2007).
[44] N. R. Claussen, S. J. J. M. F. Kokkelmans, S. T. Thompson, E. A. Donley, E. Hodby, and C. E. Wieman, Phys. Rev. A **67**, 060701(R) (2003).
[45] S. B. Papp and C. E. Wieman, Phys. Rev. Lett. **97**, 180404 (2006).
[46] T. B. Ottenstein, T. Lompe, M. Kohnen, A. N. Wenz, and S. Jochim, Phys. Rev. Lett. **101**, 203202 (2008).
[47] J. H. Huckans, J. R. Williams, E. L. Hazlett, R. W. Stites, and K. M. O'Hara, Phys. Rev. Lett. **102**, 165302 (2009).
[48] J. R. Williams, E. L. Hazlett, J. H. Huckans, R. W. Stites, Y. Zhang, and K. M. O'Hara, Phys. Rev. Lett. **103**, 130404 (2009).
[49] E. Braaten, H.-W. Hammer, D. Kang, and L. Platter, Phys. Rev. Lett. **103**, 073202 (2009).
[50] M. Suzuki, Prog. Theor. Phys. **56**, 1454 (1976).
[51] B. M. McCoy and J.-M. Maillard, Prog. Theor. Phys. **127**, 791 (2012).

Correction: The previously published Figure 3 contained an error in the legend of panel (b) and has been replaced.